



## OPEN

SUBJECT AREAS:  
STABLE ISOTOPES  
BIOGEOCHEMISTRYReceived  
23 April 2014Accepted  
3 June 2014Published  
23 June 2014Correspondence and  
requests for materials  
should be addressed to  
S.B. (steven.bouillon@  
ees.kuleuven.be)

# Contrasting biogeochemical characteristics of the Oubangui River and tributaries (Congo River basin)

Steven Bouillon<sup>1</sup>, Athanase Yambélé<sup>2</sup>, David P. Gillikin<sup>3</sup>, Cristian Teodoru<sup>1</sup>, François Darchambeau<sup>4</sup>, Thibault Lambert<sup>4</sup> & Alberto V. Borges<sup>4</sup><sup>1</sup>Department of Earth and Environmental Sciences, KULeuven, Leuven, Belgium, <sup>2</sup>Service de l'Agrométéorologie et de Climatologie, Direction de la Météorologie Nationale, Bangui, Central African Republic, <sup>3</sup>Department of Geology, Union College, Schenectady, NY, USA, <sup>4</sup>University of Liège, Chemical Oceanography Unit, Liège, Belgium.

The Oubangui is a major tributary of the Congo River. We describe the biogeochemistry of contrasting tributaries within its central catchment, with watershed vegetation ranging from wooded savannahs to humid rainforest. Compared to a 2-year monitoring record on the mainstem Oubangui, these tributaries show a wide range of biogeochemical signatures, from highly diluted blackwaters (low turbidity, pH, conductivity, and total alkalinity) in rainforests to those more typical for savannah systems. Spectral analyses of chromophoric dissolved organic matter showed wide temporal variations in the Oubangui compared to spatio-temporal variations in the tributaries, and confirm that different pools of dissolved organic carbon are mobilized during different hydrological stages.  $\delta^{13}\text{C}$  of dissolved inorganic carbon ranged between  $-28.1\text{‰}$  and  $-5.8\text{‰}$ , and was strongly correlated to both partial pressure of  $\text{CO}_2$  and to the estimated contribution of carbonate weathering to total alkalinity, suggesting an important control of the weathering regime on  $\text{CO}_2$  fluxes. All tributaries were oversaturated in dissolved greenhouse gases ( $\text{CH}_4$ ,  $\text{N}_2\text{O}$ ,  $\text{CO}_2$ ), with highest levels in rivers draining rainforest. The high diversity observed underscores the importance of sampling that covers the variability in subcatchment characteristics, to improve our understanding of biogeochemical cycling in the Congo Basin.

The recognition that carbon (C) processing within inland waters could be a substantial component in C budgets at the catchment, regional, or global scale (e.g.<sup>1–3</sup>), has led to an increased momentum in studies on riverine biogeochemistry. Further constraining the role of river systems will only be possible by generating additional comprehensive datasets, in particular on systems or regions which are currently underrepresented. Of key importance are tropical and subtropical regions, which have been suggested to be of particular importance in terms of riverine transport of sediments and carbon (e.g.<sup>4–5</sup>), and have been suggested to show higher areal  $\text{CO}_2$  outgassing rates than their temperate or boreal counterparts<sup>3,6</sup>. Based on a long tradition of interdisciplinary studies, the Amazon often serves as a model system for the biogeochemical functioning of tropical river basins with African rivers being largely neglected. The Congo River basin is second to the Amazon in terms of discharge (1310 versus 6640  $\text{km}^3 \text{yr}^{-1}$ ) and catchment size (3.8  $10^6$  versus 5.8  $10^6 \text{ km}^2$ ), but is much less well characterized from a hydrological, physico-chemical, and biogeochemical point of view. The main biogeochemical studies on the Congo basin have focussed on dissolved and particulate erosion rates both on the main Congo River and in some of its major tributaries such as the Oubangui and Sangha (e.g.<sup>7–11</sup>). The synthesis of Laraque et al.<sup>11</sup>, however, shows that sampling efforts were concentrated on a limited number of sites, and these monitoring programmes were limited to a restricted number of basic parameters. For many stations, extrapolations needed to be made based on less than 5 samples (e.g. the upper Congo River and Kasai River<sup>12</sup>). Mariotti et al.<sup>13</sup> provided the first stable isotope data on particulate organic carbon (POC) from the lower Congo River and some of its tributaries. More recently, some explorative work on the organic and inorganic C biogeochemistry of the lower Congo River has been presented<sup>14–46</sup>, and we reported results from a 1-year sampling programme on the Oubangui at Bangui (Central African Republic, CAR), focussing on the dynamics and annual export of different C pools and greenhouse gas (GHG) emissions<sup>17</sup>. Rivers in the Congo basin network, however, can be expected to show highly variable physico-chemical and biogeochemical characteristics, considering the range in geology, climatic conditions and land use/vegetation across the basin. Laraque et al.<sup>18</sup> analysed the physico-chemical properties and major ion composition in different tributaries of the lower Congo, and found strong contrasts between those draining the



“Cuvette Congolaise” (mainly rainforest-dominated lowlands) and the “Téké plateaux”, where savannahs form the main biome type. Similarly, Mann et al.<sup>19</sup> recently demonstrate strong gradients in biogeochemical characteristics across rivers and streams in the Sangha and lower Oubangui catchment. The existence of a large gradient in biogeochemical characteristics is relatively well documented for some of the large South American basins (e.g.<sup>20</sup>), but comprehensive geochemical data from the Congo basin are still mostly limited to the mainstem in the Malebo Pool at Brazzaville and some of the main tributaries. During three sampling campaigns between 2010 and 2012, we sampled a number of tributaries of the Oubangui River, from savannah-dominated systems (Mbali River, Mpoko River) to those draining mainly humid rainforest ecosystems (Lobaye, Mbaéré, Bodingué, and some of their minor tributaries) in the Ngotto Forest (Figure 1). Here, we compare biogeochemical data from these tributaries with our own results from 2 years of high-frequency sampling on the mainstem Oubangui River at Bangui, and with available literature data on the wider Congo Basin.

## Results

**Material fluxes in the Oubangui River.** A detailed discussion of results for the first year of monitoring was presented in Bouillon et al.<sup>17</sup>. While no direct DOC measurements are available for the 2<sup>nd</sup> year, we estimated DOC fluxes based on the relationship between  $a_{350}$  and DOC observed in the tributaries (see Supplement Figure S1; unpublished data from other sites within the larger Congo Basin also follow this trend). The 2<sup>nd</sup> year of measurements was characterized by a markedly lower annual discharge (~30% lower), and for most elements, the annual transport fluxes were accordingly lower than

those reported previously by 22% (for DIC) to 55% (for DOC, summarized in Table 1). As an illustration, the seasonal patterns over both years of sampling are presented in Figures 2–3 for TSM, TA,  $\delta^{13}C_{DIC}$ ,  $pCO_2$ ,  $CH_4$  and  $N_2O$ . The full data can be found in<sup>17</sup> and in Supplementary Table 2. During the 2<sup>nd</sup> year, however, we also analysed spectral parameters of cDOM. The  $a_{350}$  values exhibited a strong increase with increasing discharge, with values ranging from about  $5\text{ m}^{-1}$  during base flow to  $> 20\text{ m}^{-1}$  during high flow (Figure 4). The  $a_{250}:a_{365}$  ratio values were relatively high during base flow (4.6–5.5) and dropped markedly during the ascending limb of the hydrograph to values closed to 4.2 during high flow period (Figure 4). Opposite patterns were observed for the spectral slopes.  $S_{275-295}$  values decreased with increasing discharge (from  $>0.016\text{ nm}^{-1}$  during base flow to  $0.012\text{ nm}^{-1}$  during high flow) whereas  $S_{350-400}$  values increased with increasing discharge (from  $0.013\text{ nm}^{-1}$  during base flow to  $0.016\text{ nm}^{-1}$  during high flow). Finally, spectral slope ratios ( $S_R$ ) exhibited a strong seasonal variation with markedly higher values during base flow period ( $>1.2$ ) compared to high flow period (about 0.8).

Despite the lower transport fluxes, estimated  $CO_2$  fluxes across the water-air interface were similar or slightly higher during 2011–2012 than during 2010–2011 (Table 1). Overall, the seasonality in concentrations and isotope ratios followed similar patterns during both years (Figures 2–3), hence we will not discuss these in detail but use the data mainly to examine overall patterns across the mainstem and tributaries.

**Tributary characteristics.** Tributaries showed a much wider range of values for most of the measured variables than recorded during the

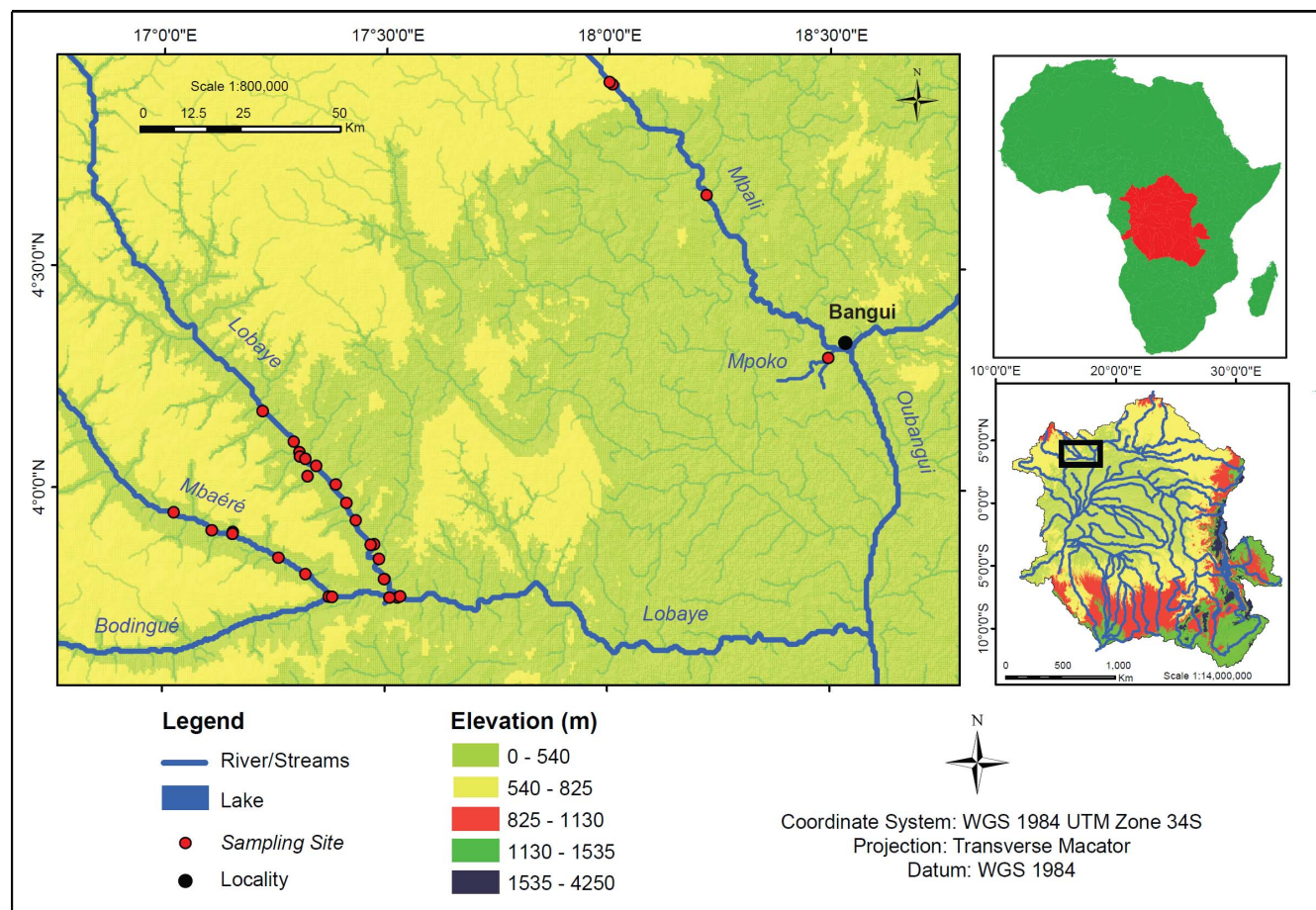


**Figure 1** | Map showing the location of the Oubangui within the Congo Basin, and detailed map showing the tributary sampling sites (note that some sites represent small first order tributaries). Map produced using ArcGIS software.



**Table 1** | Summary of fluxes and element ratios, and yields (i.e. fluxes expressed per unit area of the catchment) measured in the Oubangui River at Bangui during two subsequent hydrological years, 20th March 2010 to 19th March 2011 (data from Bouillon et al. 2012) and 20th March 2011 to 18th March 2012 (this study). Fluxes are expressed in  $\text{Tg y}^{-1}$ , yields are expressed in  $\text{ton km}^{-2} \text{y}^{-1}$

Constituent	Flux, 2010–2011	Flux, 2011–2012	Yield, 2010–2011	Yield, 2011–2012
Discharge ( $\text{m}^3 \text{s}^{-1}$ )	3361	2343		
TSM	2.45	1.63	5.01	3.33
POC	0.1446	0.0889	0.296	0.182
PN	0.0142	0.0100	0.029	0.020
DOC	0.725	0.323 <sup>a</sup>	1.483	0.661
DIC	0.479	0.374	0.980	0.765
%POC	5.9	5.5		
POC/PN (mass based)	10.2	8.9		
Annual water-air $\text{CO}_2$ flux ( $\text{mmol CO}_2 \text{m}^{-2} \text{d}^{-1}$ )	24.5 <sup>b</sup> –46.7 <sup>c</sup>	28.9 <sup>b</sup> –53.3 <sup>c</sup>		

a: estimated based on relationship between  $a_{350}$  and DOC concentrations, see text and Supplementary Figure S1. b, c: calculated using two different parameterisations, see<sup>17</sup> for details.

2 years of monitoring on the mainstem Oubangui River. Biogeochemical signatures in the tributaries appear to be clustered according to the catchment characteristics. Specific conductivity generally showed very low values (average  $14.6 \mu\text{S cm}^{-1}$ , with a minimum of  $7.6 \mu\text{S cm}^{-1}$ ) in many sites within the densely vegetated Ngotto Forest (Lobaye, Mbaéré, Bodingué), and was higher in the more northern, savannah catchments (Mbali, Mpoko:  $22\text{--}170 \mu\text{S cm}^{-1}$ ) as well as in all left bank tributaries of the Lobaye river (average  $89.4 \mu\text{S cm}^{-1}$ ) which are situated at the rainforest/savannah transition. TA was generally well correlated with specific conductivity (Figure 5), and ranged between 0.009 and  $1.791 \text{ mmol L}^{-1}$ . The highly dilute rivers in rainforest-dominated catchments were also characterised by very low TSM concentrations ( $0.7\text{--}16.0 \text{ mg L}^{-1}$ ) while higher TSM loads were encountered in some of the tributaries of the Lobaye ( $9.4\text{--}44.4 \text{ mg L}^{-1}$ ) and in Mpoko River ( $78.0 \text{ mg L}^{-1}$ ). Rivers in the Ngotto Forest were also characterized by relatively lower pH values, but despite the visual appearance as 'blackwater' rivers (in particular the Mbaéré and Bodingué), do not

show substantially higher DOC concentrations (between 1 and  $6 \text{ mg L}^{-1}$  for the majority of samples, Figure 6). The  $a_{350}$  values of the Oubangui tributaries were higher during the wet period ( $36.2 \pm 14.0 \text{ m}^{-1}$ ) than during the dry period ( $22.9 \pm 6.8 \text{ m}^{-1}$ ) (see Supplementary Tables) and are well correlated with DOC concentrations across the seasons (Figure S1). The variations of  $a_{250}:a_{365}$  ratios were relatively limited within and across seasons, with a pattern of lower values during wet period ( $3.84 \pm 0.16$ ) compared to the dry period ( $4.02 \pm 0.17$ ). Spectral slopes over the range 275–295 nm ( $S_{275-295}$ ) decreased weakly between the dry and wet period, with mean values of  $0.0124 \pm 0.0004 \text{ nm}^{-1}$  and  $0.0116 \pm 0.0003 \text{ nm}^{-1}$ , respectively. In contrast,  $S_{350-400}$  values tended to be higher during wet period ( $0.0152 \pm 0.001 \text{ nm}^{-1}$ ) compared to dry period ( $0.0147 \pm 0.0009 \text{ nm}^{-1}$ ). The difference in the  $S_R$  ratio was however more marked between the two seasons, with lower values during the wet period ( $0.770 \pm 0.049$ ) compared to the dry period ( $0.845 \pm 0.046$ ). Note that the variations of DOM composition proxies were more marked when data are compared site to site. For example, the increase in  $a_{350}$  in the Mbaéré from 10.5 to  $35.0 \text{ m}^{-1}$  between dry and wet periods was related to clear decreases in the  $a_{250}:a_{365}$  ratio (from 4.3 to 3.7),  $S_{275-295}$  (from 0.0131 to  $0.0117 \text{ nm}^{-1}$ ) and  $S_R$  (from 0.860 to 0.799). Compared to the mainstem Oubangui River,  $\delta^{13}\text{C}$  values of DIC span a wide range of values and are typically more  $^{13}\text{C}$ -depleted, with very low values in the Mbaéré ( $-23.5 \pm 2.0\text{‰}$ ), intermediate values in the mainstem Lobaye ( $-16.1 \pm 2.0\text{‰}$ ) and in its minor tributaries ( $-14.3 \pm 2.3\text{‰}$ ), and highest values in the Mbali and Mpoko River ( $-11.1$  to  $-10.5\text{‰}$ ).  $\delta^{13}\text{C}_{\text{DIC}}$  values are strongly negatively correlated with  $\text{pCO}_2$  (Figure 7). With the exception of the Mpoko River,  $\delta^{13}\text{C}$  values of POC and DOC fall within the range expected for a dominance of C3 vegetation ( $-31.2$  to  $-25.8\text{‰}$  for POC,  $-30.6$  to  $-27.0$  for DOC). The more turbid Mpoko River showed a  $\delta^{13}\text{C}_{\text{POC}}$  of  $-22.8\text{‰}$ , indicating a substantial contribution from C4 vegetation in this subcatchment (no  $\delta^{13}\text{C}_{\text{DOC}}$  data available for this site).  $\delta^{13}\text{C}$  values of POC and DOC pools were well correlated, and  $\delta^{13}\text{C}_{\text{POC}}$  values increased with TSM load (Figure 8).

Calculated  $\text{pCO}_2$  values for the different Oubangui tributaries were highly variable, ranging between 870 and 33500 ppm, being generally higher than those observed in the mainstem Oubangui River (Figure 9). Similarly, both dissolved  $\text{CH}_4$  and  $\text{N}_2\text{O}$  concentrations were generally higher in tributaries than in the mainstem Oubangui River (Figure 9).

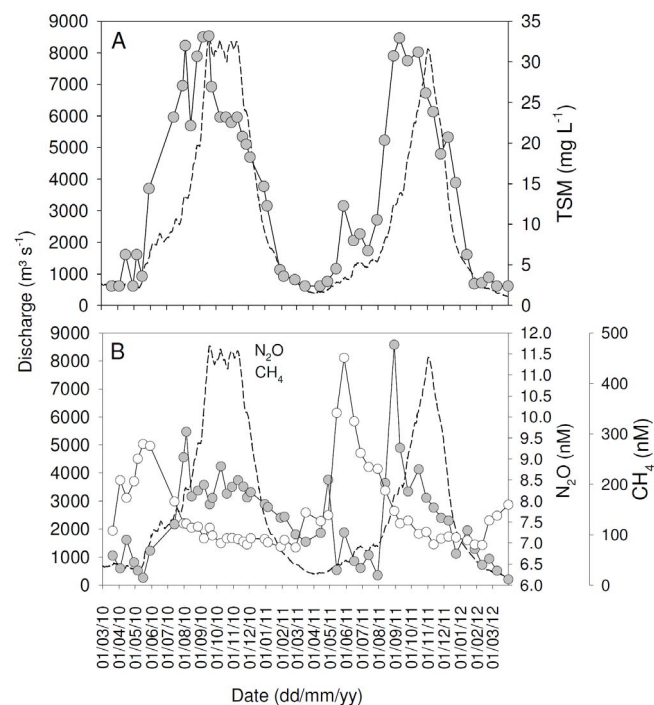


**Figure 2** | Seasonal variations of daily discharge (dotted lines) and (A) total suspended matter concentrations (TSM), and (B) concentrations of  $\text{CH}_4$  and  $\text{N}_2\text{O}$  in the Oubangui River at Bangui between March 2010 and March 2012.

## Discussion

**Organic carbon.** Rivers are often categorized in one of three types, mainly based on colour, distinguishing white-water rivers (alkaline to neutral pH, high sediment loads), black-water rivers (acidic, high DOC loads, very low sediment loads and dissolved ion concentrations), and clear-water rivers (low sediment loads but

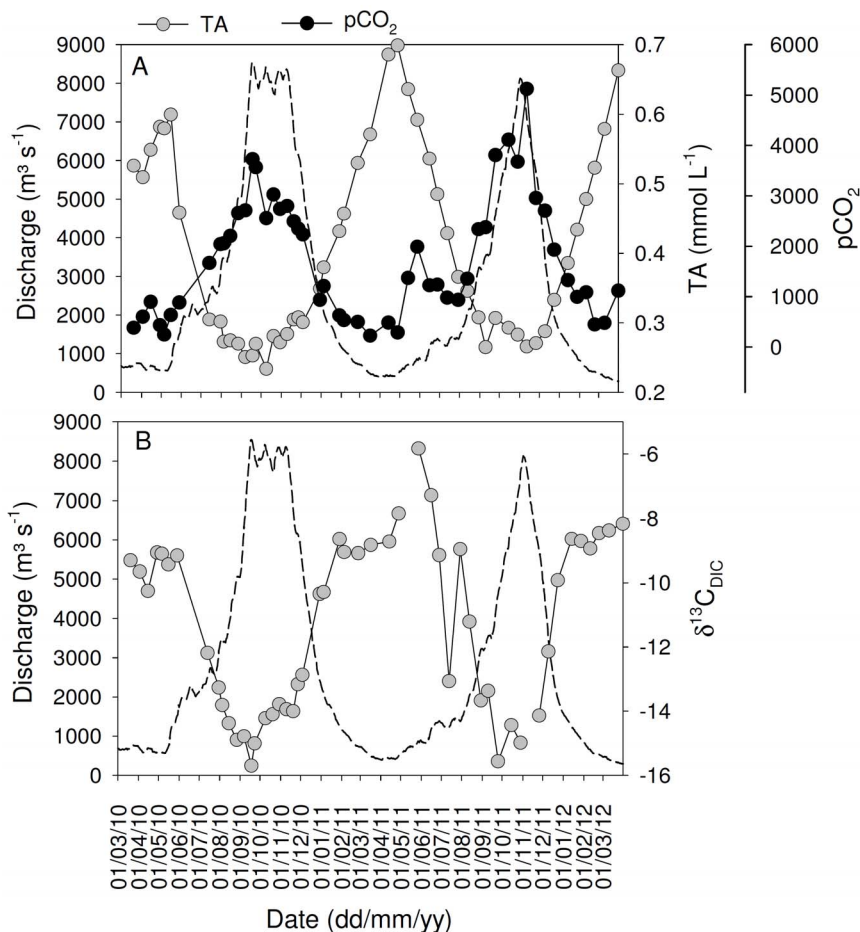


**Figure 3** | Seasonal variations of daily discharge (dotted lines) and (A) total alkalinity (TA) and the partial pressure of CO<sub>2</sub> (pCO<sub>2</sub>), and (B) the carbon stable isotope signatures of dissolved inorganic carbon ( $\delta^{13}\text{C}_{\text{DIC}}$ ) in the Oubangui River at Bangui between March 2010 and March 2012.

variable in terms of pH and alkalinity). This distinction is, however, not always straightforward (see e.g. 21). Consistent with the generally low mechanical erosion rates reported for the Congo Basin<sup>11</sup>, TSM concentrations in most of the tributaries were low. Only the Mpoko River which drains a wooded savannah region and some of the minor tributaries of the Lobaye, on the rainforest-savannah transition zone, showed slightly more elevated TSM concentrations (9.0–78.0 mg L<sup>-1</sup>). While the Bodingué and Mbaéré watersheds sampled here visually show characteristics of blackwater rivers, their DOC concentrations (1.5–7.1 mg L<sup>-1</sup>) in the lower range of those found

in the mainstem Oubangui (Figure 8), and generally lower than those reported for the mainstem Congo River (6.2 to 17.6 mg L<sup>-1</sup>; 13,19) or the Epulu River in the upper Congo Basin (5.2–9.0 mg L<sup>-1</sup>; Spencer et al. 2010), and lower than the range reported for blackwater rivers in the Amazon (7–40 mg L<sup>-1</sup>, 21). In all of the sampled tributaries, DOC remained the dominant form of organic C (OC), representing 53–95% of the total OC pool. While sampling sites were not consistently similar between different sampling campaigns, DOC concentrations were generally higher during the 2012 wet season compared to the 2 dry season campaigns (e.g. for the mainstem Lobaye:  $3.5 \pm 0.9$  mg L<sup>-1</sup>, n=5 during the wet season,  $1.9 \pm 0.1$  mg L<sup>-1</sup>, n=5 during dry season; for the Mbaéré:  $6.4 \pm 1.0$  mg L<sup>-1</sup>, n=2 during the wet season,  $2.4 \pm 0.8$  mg L<sup>-1</sup>, n=6 during dry season). Such higher DOC concentrations during wet conditions are in line with results from other sites in the Congo basin such as the mainstem Oubangui<sup>10,17</sup>, mainstem Congo<sup>10,16</sup>, and rivers in the Ituri Forest<sup>14</sup>.

The ratio of spectral slopes  $S_R$  and the  $a_{250}:a_{365}$  ratio were developed as rapid and easy methods for characterizing cDOM. The  $S_R$  ratio has been correlated to molecular weight and sources, i.e. samples of greater allochthonous contribution with higher molecular weight DOM have lower  $S_R$  values<sup>22</sup>. The  $a_{250}:a_{365}$  ratio has been correlated with the molecular size and DOM aromaticity with decreasing values relating to increasing molecular size<sup>23</sup>. In a recent study focusing on cDOM properties in 30 U.S. Rivers, Spencer et al.<sup>24</sup> also showed that the  $a_{250}:a_{365}$  ratio was inversely related to the hydrophobic organic acid fraction (HPOA) of DOM which represents the high molecular weight, aromatic-dominated fraction of DOM<sup>25</sup>. Therefore, low  $a_{250}:a_{365}$  ratio values (high HPOA fraction)

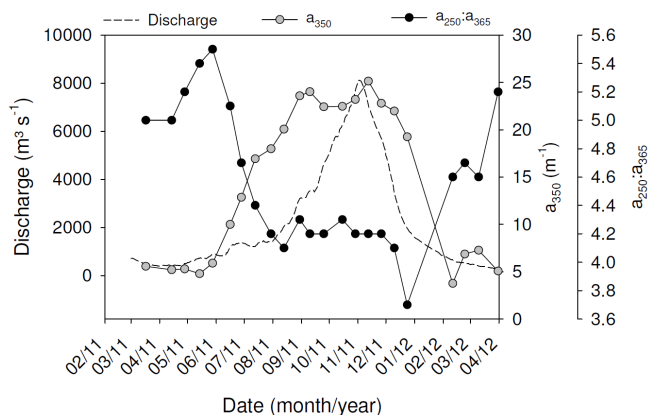


**Figure 4** | Seasonal variations of  $a_{350}$  and the  $a_{250}:a_{365}$  ratio in the mainstem Oubangui River between March 2011 and April 2012.

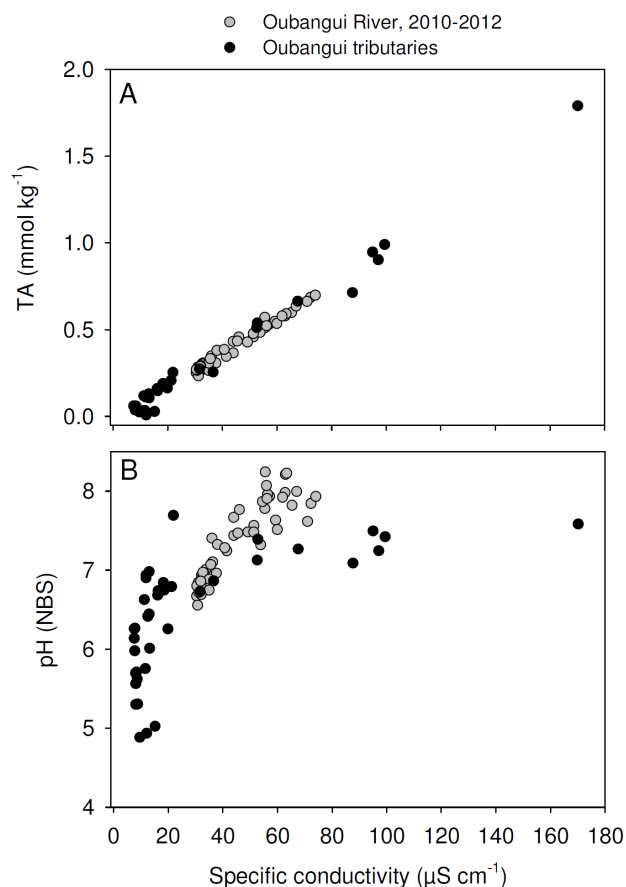


**Figure 5** | Relationships between specific conductivity and (A) total alkalinity (TA), and (B) in situ pH for the mainstem Oubangui (grey circles; data from 2 years of monitoring), and tributaries of the Oubangui (black circles).

indicate an allochthonous origin of DOM, whereas high  $a_{250}:a_{365}$  values (low HPOA fraction) suggest an autochthonous source (algal or microbial) or photodegraded DOM<sup>26–27</sup>.

The ranges of  $S_{275-295}$ ,  $S_{350-400}$  and  $S_R$  in the Oubangui system are comparable to that from other allochthonous dominated freshwater systems including temperate, Arctic, and tropical rivers<sup>15,22,28–30</sup>. The range of the  $a_{250}:a_{365}$  ratio is comparable to that from other temperate and Arctic rivers<sup>15,28</sup>.

The large variations in stream  $S_R$  and  $a_{250}:a_{365}$  ratios that occurred along with changes in DOC concentrations and water discharge during the high flow period in the Oubangui River and its tributaries clearly indicate that DOM pools are being mobilized that are different than those typical of base flow conditions (Supplementary Tables 4 and 5). Similar changes in DOM optical properties across the hydrological cycle, especially in spectral slopes proxies, have also been reported in tropical<sup>14,29</sup> and Arctic rivers<sup>28,30</sup>, as well as in an agricultural watershed in California<sup>31</sup>. Highest DOC concentrations were linked with lower  $S_R$  and  $a_{250}:a_{365}$  values, indicating an increase in the contribution of allochthonous sources to stream DOM due to greater surface runoff and leaching of organic rich layers during the high flow period<sup>14,30</sup>. However, lowest DOC concentrations were linked with higher  $S_R$  and  $a_{250}:a_{365}$  values, indicating that DOM is less aromatic in nature during the base flow period. This shift in DOM sources can be explained by the deepening of hydrologic flow paths through the soil profile and greater residence time of DOC in contact with soil subsurface microbial communities, leading to the mobilization of a more microbially processed DOM during base flow period<sup>14,30</sup>. However, combining optical and fluorescence properties of cDOM, Yamashita et al.<sup>29</sup> proposed another explanation in the

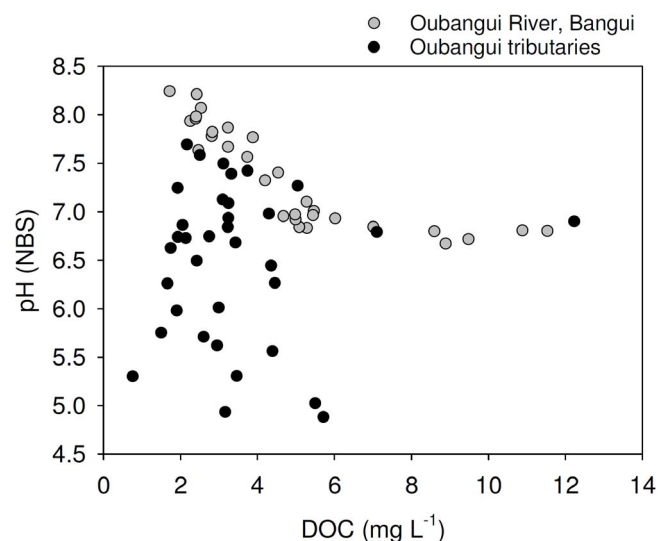


**Figure 6** | Relationship between dissolved organic carbon (DOC) concentrations and in situ pH for the mainstem Oubangui (grey circles; data from 2 years of monitoring), and tributaries of the Oubangui (black circles).

interpretation of the increase of  $S_R$  during base flow period reported in tropical rivers in Venezuela. These authors suggested that the increase of  $S_R$  values could potentially result from a higher contribution of autochthonous source by enhanced plankton primary productivity during the low turbidity period. However, based on the previous study of Bouillon et al.<sup>17</sup>, such autochthonous source has not been identified as contributor of DOC in the Oubangui River, supporting the hypothesis of a deepening of hydrological flow path as driver of changes in DOM sources.

The temporal variation observed in spectral slopes proxies in the Oubangui River are similar to those observed in the Epulu River<sup>14</sup>. During the wet period (April) the Epulu was characterized by lowest  $S_R$  values ( $0.834 \pm 0.028$ ) close to those measured in the Oubangui River during high flow period occurring from September to December ( $0.832 \pm 0.041$ ). In the Epulu River,  $S_R$  increased with decreasing discharge during post- and intermediary periods (November–February), with mean and maximal values of  $0.962 \pm 0.056$  and 1.066, respectively. Mean value of  $S_R$  in the Oubangui River

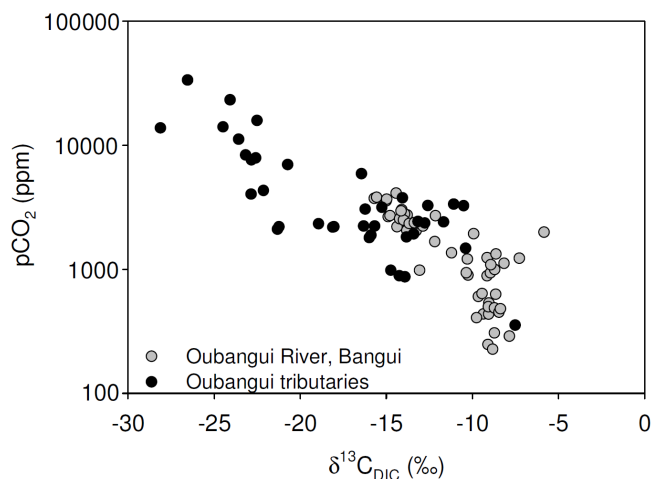


**Figure 7** | Relationships between the carbon stable isotope composition of DIC ( $\delta^{13}C_{DIC}$ ) and the partial pressure of  $CO_2$  ( $pCO_2$ ), for the mainstem Oubangui (grey circles; data from 2 years of monitoring), and tributaries of the Oubangui (black circles).

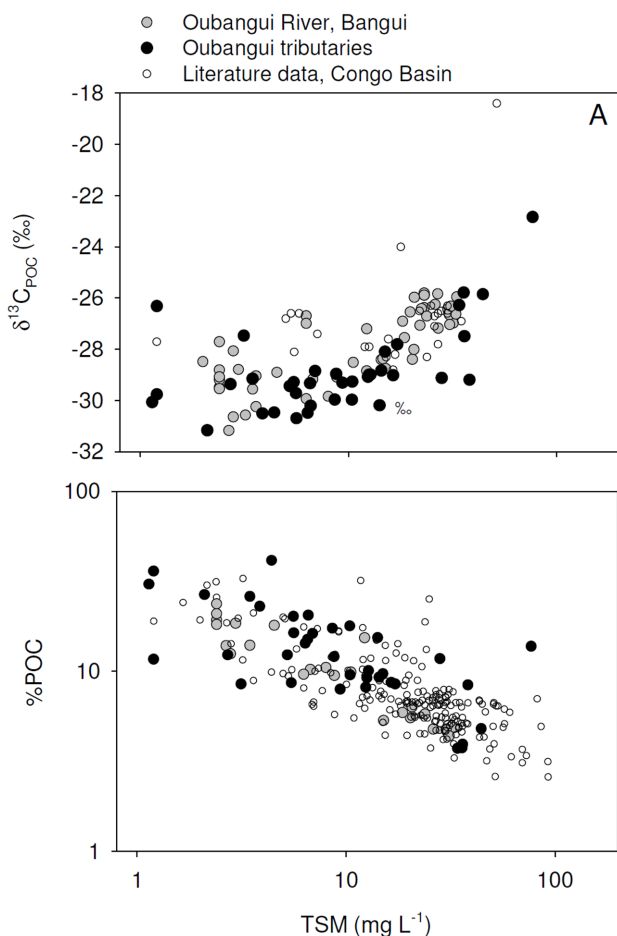


**Figure 8** | Relationship between total suspended matter concentrations (TSM) and (a)  $\delta^{13}\text{C}$  signatures of particulate organic carbon ( $\delta^{13}\text{C}_{\text{POC}}$ ), and (b) the contribution of particulate organic carbon (POC) to the TSM pool (%POC) for the mainstem Oubangui, tributaries of the Oubangui and samples collected throughout the Congo basin (literature data from Mariotti et al. 1991, Sigha-Nkamdjou et al. 1993, Coynel et al. 2005, Bouillon et al. 2012, Spencer et al. 2012).

during base flow periods was higher, about  $1.180 \pm 0.116$ , with a maximal  $S_R$  value of 1.323.  $S_{350-400}$  values showed the same temporal variations in both rivers, with lowest values in the Oubangui River compared to the Epulu River. The main difference between these two tropical rivers is the variations in  $S_{275-295}$  values observed in the Oubangui River and to a lower extent in Oubangui tributaries. High flow period was associated with a clear decrease in  $S_{275-295}$ , whereas Spencer et al.<sup>14</sup> reported no seasonal variations in  $S_{275-295}$  across the hydrological cycle.

Despite the similar temporal variations in DOC concentrations and DOM composition, spatial differences can be observed between the Oubangui River and its tributaries. The Oubangui River is characterized by a more important range of variations in whole cDOM parameters, including absorption coefficient,  $a_{250}:a_{365}$  (E2:E3), and spectral slope coefficients. This observation is quite different from those reported by Yamashita et al.<sup>29</sup>, where hydrological changes seem to affect cDOM properties in tributaries to a larger extent than the main river channels.

$\delta^{13}\text{C}_{\text{POC}}$  values showed a positive correlation with sediment loads (Figure 8), but were generally in the range expected for C3-dominated catchments. The  $\delta^{13}\text{C}$  values in the rivers draining the Ngotto Forest are relatively low ( $-32.2$  to  $-29.1\%$ ), but vegetation in these systems can be expected to have low  $\delta^{13}\text{C}$  values given the effects of

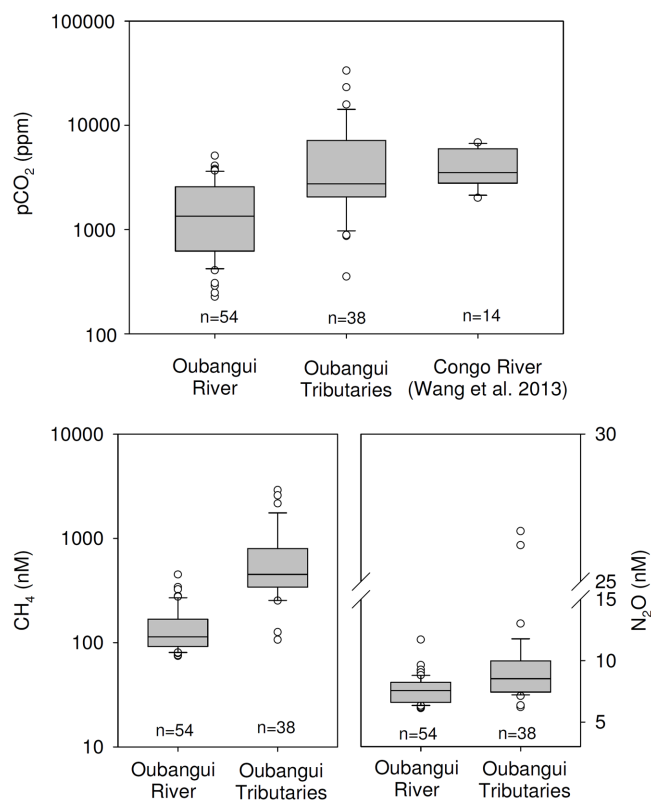


**Figure 9** | Boxplots of data on  $\text{pCO}_2$ ,  $\text{CH}_4$ , and  $\text{N}_2\text{O}$  concentrations for the mainstem Oubangui River (data from 2 years of monitoring), and tributaries of the Oubangui (all sites and sampling seasons combined).  $\text{pCO}_2$  data for the lower Congo River are from Wang et al. (2013).  $n$  indicates the number of data points.

both high precipitation<sup>32</sup> and relatively closed-canopy structure (e.g.,<sup>33</sup>). The increasing pattern in  $\delta^{13}\text{C}_{\text{POC}}$  values with increased sediment loads (albeit still low on a global scale, 34) suggests higher sediment inputs in catchments where C4 vegetation is more substantial (i.e., from savanna landscapes). The negative relationship between TSM loads and %POC (the contribution of POC to the total particulate matter load, Figure 8) has been previously observed in a range of individual river basins (e.g.,<sup>35</sup>), and on a global scale (e.g.,<sup>4,36</sup>). In our case, this correlation can be interpreted as reflecting the continuum from 2 contrasting end-members: (i) direct litter or organic-rich surface soil layers as observed in the majority of the rainforest rivers, and (ii) more soil-derived sediments as observed in the more turbid systems, with correspondingly lower %POC.

**Inorganic carbon.**  $\text{HCO}_3^-$  in rivers is mainly derived from the weathering of carbonate and silicate rocks, with the relative proportions depending to a very large extent on the lithology of the drainage basin<sup>37-38</sup>. Gaillardet et al. (39, based on data from 8) estimated the relative contributions of carbonate and silicate weathering to the bicarbonate load of the Congo River and some of its tributaries (Oubangui, Sangha, and Kasai) and found a contribution of silicate weathering generally between 50–60% except for the Sangha where carbonate dissolution dominated (only 9% resulting from silicate weathering). Since we do not have data on  $\text{Cl}^-$  concentrations as required in their approach, we used the simple stoichiometric model of Garrels and Mackenzie<sup>37</sup> whereby the contribution to TA from carbonate weathering ( $\text{TA}_{\text{carb}}$ ) is computed from  $\text{Ca}^{2+}$  and  $\text{Mg}^{2+}$  concentrations and the contribution to TA from silicate weathering ( $\text{TA}_{\text{sil}}$ ) is computed independently from dissolved silicon (Si) concentrations, according to:

$$\text{TA}_{\text{carb}} = 2 * ([\text{Ca}^{2+}] + [\text{Mg}^{2+}] - [\text{SO}_4^{2-}])$$

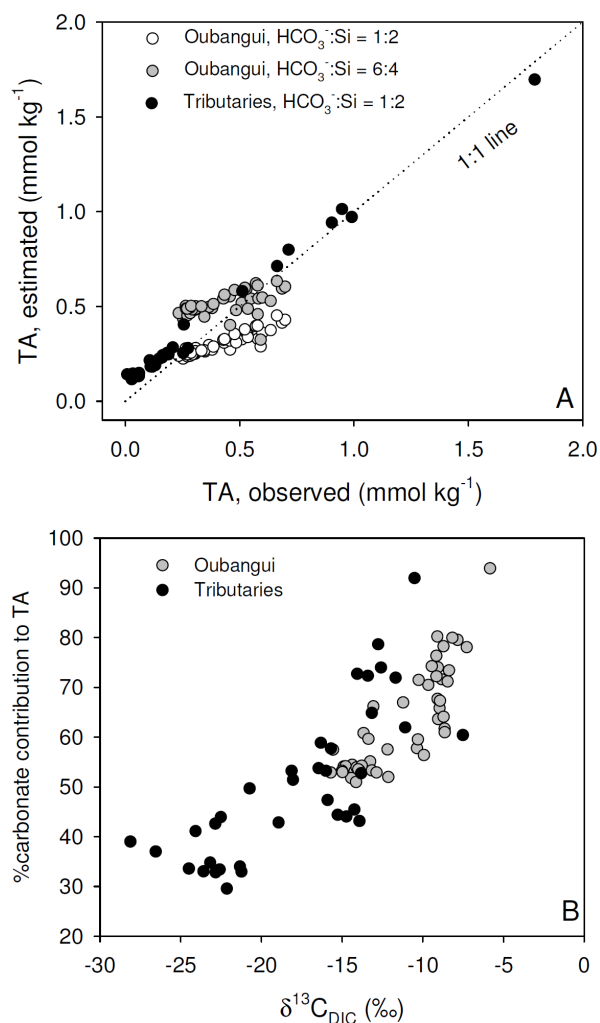


**Figure 10** | Relationship between (A) observed and modeled total alkalinity (TA) (see text for details), and (B) the carbon stable isotope composition of DIC ( $\delta^{13}\text{C}_{\text{DIC}}$ ) and the estimated contribution of TA derived from carbonate weathering to the observed TA.

$$\text{TA}_{\text{sil}} = [\text{Si}]/2$$

$\text{SO}_4^{2-}$  allows to account for  $\text{Ca}^{2+}$  originating from the dissolution of gypsum ( $\text{CaSO}_4$ ), but this correction term was ignored in absence of  $\text{SO}_4^{2-}$  data. In a companion study in the Tana basin (Kenya) we found  $\text{SO}_4^{2-}$  to correspond to about 10% of  $\text{Ca}^{2+}$  for a variety of streams and rivers<sup>40</sup>, which is likely an upper estimate for our study area given the more humid climate and the absence of evaporative environments.

For the tributaries, there is a good linear regression between the modeled TA ( $\text{TA}_{\text{carb}} + \text{TA}_{\text{sil}}$ ) and observed TA ( $r^2 = 0.99$ ,  $n = 36$ , Figure 10A). In the Oubangui mainstem, the modeled TA is well correlated to the observed TA but markedly deviates from the 1:1 line as the values increase. The stoichiometric model of<sup>37</sup> assumes that the weathering of silicate rocks leads to a release of  $\text{HCO}_3^-$  and dissolved Si (DSi) according to a 1:2 ratio. This is true for common mineral forms such as olivine and albite, but the dissolution of some other mineral forms lead to a different  $\text{HCO}_3^-$ :DSi ratio. For instance, the weathering of plagioclase feldspar ( $\text{NaCaAl}_3\text{Si}_5\text{O}_{16}$ ) leads to the release of  $\text{HCO}_3^-$  and DSi in a 6:4 ratio. While no detailed information is available on the mineralogy of the underlying bedrock in our study catchments, they are underlain mostly by metamorphic rocks in which feldspars are likely to be common constituents. When we apply this ratio to the Oubangui mainstem data, the recomputed modeled TA in the high values range is in better agree-

ment with observed TA, than based on the  $\text{HCO}_3^-$ :DSi ratio of 1:2 (Figure 10A). The contribution of carbonate rock weathering ( $\%\text{TA}_{\text{carb}}$ ) was estimated as the percentage of  $\text{TA}_{\text{carb}}$  to total modeled TA ( $\text{TA}_{\text{carb}} + \text{TA}_{\text{sil}}$ ), and ranged between 30% and 94%, encompassing the range of  $\%\text{TA}_{\text{carb}}$  computed by Gaillardet et al.<sup>39</sup> between 40% and 91%.  $\%\text{TA}_{\text{carb}}$  is positively correlated to TA indicating a lower contribution of carbonate rock weathering in the basins draining humid forest than savannah.

Carbon in  $\text{HCO}_3^-$  originating from silicate rock weathering comes exclusively from  $\text{CO}_2$ , while 1/2 of the C in  $\text{HCO}_3^-$  from carbonate rock comes from  $\text{CaCO}_3$  and the other 1/2 from  $\text{CO}_2$ . If the  $\text{CO}_2$  involved in the weathering comes from organic C degradation,  $\delta^{13}\text{C}_{\text{DIC}}$  should have a negative signature (as indicated by the  $\delta^{13}\text{C}$  signatures of DOC and POC), while marine  $\text{CaCO}_3$  has a  $\delta^{13}\text{C}$  signature close to 0‰<sup>41</sup>.

This can explain the positive relationship between  $\%\text{TA}_{\text{carb}}$  and  $\delta^{13}\text{C}_{\text{DIC}}$  (Figure 10B). When applying a linear fit to these data ( $R^2=0.69$ ), the extrapolated  $\delta^{13}\text{C}_{\text{DIC}}$  values for the end members where the contribution of carbonate weathering is 0 and 100% are  $-31.3$  and  $-1.5$ ‰, respectively, which corresponds well with the expected values for terrestrial vegetation in the rainforest biome and marine carbonates.  $\delta^{13}\text{C}_{\text{DIC}}$  values as low as those found in some of the Ngotto forest rivers (as low as  $-28.1$ ‰) have, to the best of our knowledge, only been reported for a few rivers in the Amazon basin<sup>42–43</sup>, and can only occur under conditions when alkalinity is extremely low and hence where silicate weathering dominates. The strong correlation between  $\delta^{13}\text{C}_{\text{DIC}}$  and  $\text{pCO}_2$  (Figure 7) on the one hand, and the link between  $\delta^{13}\text{C}_{\text{DIC}}$  and carbonate weathering discussed above, suggest that the relative importance of silicate versus carbonate weathering may exert an important control on  $\text{pCO}_2$  in the studied river systems. Such a mechanism is further suggested by the highly significant regressions ( $p < 0.0001$ ) between  $\log(\text{pCO}_2)$  and the estimated contribution of carbonate weathering to TA ( $R^2=0.38$ ), or with Si/ $\text{Ca}^{2+}$  ratios ( $R^2=0.35$ ), i.e., rock weathering would explain close to 35% of the variance of  $\text{pCO}_2$ . A recent analysis of factors controlling inorganic carbon speciation in North American rivers<sup>44</sup> concluded that while much of the variation in the spatial patterns of TA and pH can be explained by catchment processes and characteristics related to chemical weathering (e.g., precipitation, proportion of carbonate rocks), spatial variations in  $\text{pCO}_2$  were mainly governed by in-river processes only indirectly related to the catchments (e.g. temperature through its effect on respiration). At the scale of our study, where factors such as temperature are much more homogeneous spatially and seasonally, it appears that the weathering regime could exert a partial control on the inorganic carbon speciation, and hence influence  $\text{pCO}_2$  and water-atmosphere  $\text{CO}_2$  exchange. It should be noted, however, that our calculated  $\text{pCO}_2$  data from rivers with low pH are likely to be overestimates, since a comparison of calculated  $\text{pCO}_2$  data with those measured in the field with a direct headspace technique suggests that the former approach induces a substantial bias towards higher  $\text{pCO}_2$  under conditions of low pH ( $< 6.5$ ) and/or very low TA (Abril et al., in preparation). While this compromises some of the absolute  $\text{pCO}_2$  data from rivers in the Ngotto forest, it is unlikely to distort the overall patterns described above.

**Methane and nitrous oxide.** The data compilation by Bastviken et al.<sup>2</sup> demonstrated the lack of  $\text{CH}_4$  flux data from tropical systems, despite the fact that tropical freshwater systems are often claimed to show much higher  $\text{CH}_4$  emissions than temperate or high-latitude systems. For the Oubangui tributaries, we have made no attempts to calculate diffusive  $\text{CH}_4$  fluxes (due to the lack of data required to estimate gas exchange velocities, as outlined above for  $\text{CO}_2$ ), yet it is evident that dissolved  $\text{CH}_4$  concentrations are, on average, more than an order of magnitude higher than in the mainstem Oubangui River (Figure 9). Riverine  $\text{CH}_4$  concentrations



in the few African catchments studied so far range drastically, with reported values between 1 and 6730 nM in the Athi-Galana-Sabaki River<sup>45</sup>, between 48 and 870 nM in the Comoé, Bia and Tanoé rivers in Ivory Coast<sup>46</sup>, and between 25 and 505 nM in the Tana River basin<sup>47</sup>. While CH<sub>4</sub> concentrations in the mainstem Oubangui show a pronounced seasonality (17, and Figure 2), a comparison of CH<sub>4</sub> data for the Lobaye and Mbaéré between our dry and wet season campaigns shows no distinct differences. While the riverine network is clearly a consistent source of CH<sub>4</sub> to the atmosphere, the data suggest that diffusive CH<sub>4</sub> fluxes are highly variable in space and time and therefore difficult to upscale reliably. As reported earlier for the mainstem Oubangui River, dissolved N<sub>2</sub>O levels were generally low (6.4–13.0 nM, except for the Kélé, a small and shallow rainforest stream draining into the Mbaéré where N<sub>2</sub>O concentrations reached 26.7 and 26.2 nM during the 2012 and 2013 sampling campaigns, respectively). These values represent only a slight oversaturation with respect to atmospheric equilibrium (137 ± 22%, 380–402% for the Kélé). A synthesis by Baulch et al.<sup>48</sup> found higher N<sub>2</sub>O emissions to be associated with increasing N inputs, hence the low N<sub>2</sub>O concentrations observed are in line with the pristine status of our study catchments and the observed low nitrate levels (median of 7.1 μM, range: 0–50 μM, n = 32; own unpublished data).

**Concluding remarks.** Overall, our results demonstrate that even within a relatively small set of subcatchments of the Oubangui River, biogeochemical characteristics of different rivers and streams show highly contrasting characteristics on the one hand, yet consistent co-variations between parameters on the other hand. According to Raymond et al.<sup>3</sup> and Regnier et al.<sup>49</sup>, one of the factors limiting our ability to better constrain the role of rivers in regional and global C budgets is that the current empirical database is too sparse to adequately resolve the diversity of soil types, inland waters, estuaries and coastal systems, and specifies the Congo Basin as one of the key areas of regional priority. The data collected and compiled here, while covering only a small subset of the Congo Basin, suggest that large data collection efforts will be required to adequately describe the aquatic biogeochemical variability for this large tropical basin. However, the systematic co-variation between some of the examined proxies of C origin and transformation, and the apparent link with certain catchment characteristics (lithology and vegetation) provide some important clues on the type of classification and characterization needed to upscale future data to the catchment scale.

## Methods

The Oubangui River (Figure 1) is the second largest tributary of the Congo River (after the Kasai), with a length of 2400 km from the source (Uele River) to its confluence with the Congo River, and a drainage basin of 644000 km<sup>2</sup>, of which 489000 km<sup>2</sup> (76%) is located upstream of Bangui<sup>10</sup>. The Oubangui catchment upstream of Bangui is dominated by dry wooded savannahs, with more humid forest situated downstream towards the confluence with the Congo mainstem. The mean annual precipitation in the catchment is ~1400–1540 mm y<sup>-1</sup><sup>10</sup>. The hydrological cycle of the Oubangui is characterized by a single main flood peak and maximum discharge typically in October–November. Annual discharge has fluctuated between 2120 m<sup>3</sup> s<sup>-1</sup> (1990) and 6110 m<sup>3</sup> s<sup>-1</sup> (1969). Although we did not find land-use data specifically for the Oubangui catchment, deforestation rates in the CAR are reported to be among the lowest in Africa (net deforestation of 0.06% y<sup>-1</sup><sup>50</sup>). According to the Food and Agriculture Organisation (FAO) statistics (<http://faostat.fao.org/>), agricultural land use has remained stable between 1961 and 2010, and makes for ~8% of the total land area. Considering a national population density of ~7 inhabitants km<sup>-2</sup>, these figures support classifying the Oubangui catchment as nearly pristine. Monitoring on the Oubangui in the city of Bangui (CAR, 4°21' N, 18° 34' E) was initiated in late March 2010, and was followed by approximately 2-weekly sampling. A subset of data collected between March 2010 and March 2011 were presented in<sup>21</sup>; data on the subsequent year of monitoring (after which this programme ended) are included here.

Tributaries of the Oubangui were sampled in March 2010 (dry season), March 2011 (dry season), and November 2012 (wet season). During the first field campaign, two sites were sampled along the Mbali River (Fig. 1), as well as the Mpoko River just south of Bangui (see also 13), and the main rivers draining the Ngotto Forest, Lobaye

province (Fig. 1). The Ngotto Forest was revisited in 2011 and 2012 for more extensive sampling on the main rivers (Mbaéré, Lobaye, and Bodingué) and some of their minor tributaries. The Ngotto Forest, bordering on the Republic of Congo (a.k.a. Congo Brazzaville) and characterized by annual precipitation of ~1600 mm, is classified as a semi-deciduous rainforest and lies south of the wooded savannahs of the Guinea-Sudanian transition zone. Water levels were lower during the dry season surveys (March) than during the wet season (November), but water level differences are rather small (1.0–1.5 m), in line with the relatively stable discharge of the Lobaye River (monthly average flow ranging between 250 and 500 m<sup>3</sup> s<sup>-1</sup> for the period 1950–1984; data from the Global River Discharge Database (<http://www.sage.wisc.edu/riverdata/>, accessed February 2014)). The Mbaéré and Bodingué are the two main permanent rivers, which are bordered by extensive areas of seasonally flooded forests. The Bodingué River joins the Mbaéré River prior to joining the Lobaye River, which lies on the northern side of the Ngotto Forest and represents the border towards drier, savannah landscapes to the North. The Lobaye River is an important tributary of the Oubangui River. The Ngotto Forest forms a protected area with high biodiversity, and very low human population densities<sup>51</sup>. The geology of the region is complex and includes igneous, metamorphic, and Mesoproterozoic– Neoproterozoic sedimentary formations that include calcareous sediments<sup>52</sup>.

Water temperature, conductivity, dissolved oxygen (O<sub>2</sub>) and pH were measured in situ with a YSI ProPlus multimeter, whereby the O<sub>2</sub> and pH probes were calibrated on each day of data collection using water saturated air and United States National Bureau of Standards buffer solutions (4 and 7), respectively. All sampling for larger rivers was performed from dugout canoes at ~0.5 m below the water surface, in a few cases sampling was performed from a bridge (Mpoko) or from the river shore (Mbali). Samples for dissolved gases (CH<sub>4</sub>, N<sub>2</sub>O) and the stable isotope composition of dissolved inorganic C (δ<sup>13</sup>C<sub>DIC</sub>) were collected with a Niskin bottle or a custom-made sampling bottle consisting of an inverted 1L polycarbonate bottle with the bottom removed, and ~0.5 m of tubing attached in the screw cap<sup>53</sup>. 12 mL exetainer vials (for δ<sup>13</sup>C<sub>DIC</sub>) and 50 mL serum bottles (for CH<sub>4</sub> and N<sub>2</sub>O) were filled from water flowing from the outlet tubing, poisoned with HgCl<sub>2</sub>, and capped without headspace. Approximately 2000 mL of water were collected 0.5 m below the water surface for other particulate and dissolved variables, and filtration and sample preservation was performed in the field within 2 h of sampling.

Samples for total suspended matter (TSM) were obtained by filtering 200–1000 mL of water on pre-combusted (4 h at 500°C) and pre-weighed glass fiber filters (47 mm GF/F, 0.7 μm nominal pore size), and dried in ambient air during the fieldwork. Samples for determination of particulate organic C (POC), particulate nitrogen (PN) and C isotope composition of POC (δ<sup>13</sup>C<sub>POC</sub>) were collected by filtering 50–300 mL of water on pre-combusted 25 mm GF/F filters (0.7 μm nominal pore size). The filtrate from the TSM filtrations was further filtered on 0.2 μm polyethersulfone syringe filters (Sartorius, 16532-Q) for total alkalinity (TA), DOC and δ<sup>13</sup>C<sub>DOC</sub> (8–40 mL glass vials with Polytetrafluoroethylene coated septa). TA was analysed by automated electro-titration on 50 mL samples with 0.1 mol L<sup>-1</sup> HCl as titrant (reproducibility estimated as typically better than ± 3 μmol kg<sup>-1</sup> based on replicate analyses). The partial pressure of CO<sub>2</sub> (pCO<sub>2</sub>) and DIC concentrations were computed from pH and TA measurements using thermodynamic constants of Millero<sup>54</sup> as implemented in the CO2SYS software<sup>55</sup>. It should be noted, however, that this approach is expected to overestimate pCO<sub>2</sub> in some of the blackwater rivers (see Discussion).

For the monitoring data on the Oubangui River, CO<sub>2</sub> exchange with the atmosphere was calculated as  $F = k\alpha\Delta p\text{CO}_2$  where  $k$  is the gas transfer velocity,  $\alpha$  is the solubility coefficient for CO<sub>2</sub>, and  $\Delta p\text{CO}_2$  represents the difference in partial pressure of CO<sub>2</sub> between water and air. Monthly averages corresponding to time of sampling of atmospheric pCO<sub>2</sub> from Mount Kenya (Kenya, -0.05°N 37.80°E) were retrieved GLOBALVIEW-CO2 database (Carbon Cycle Greenhouse Gases Group of the National Oceanic and Atmospheric Administration, Earth System Research Laboratory).  $k$  values were calculated using two approaches, one based on the relationship between wind speed and  $k_{600}$  (i.e.,  $k$  normalized to a constant temperature of 20°C), and an alternative approach using a gas transfer parameterization based on depth and water current that was developed for rivers and streams; details can be found in Bouillon et al.<sup>17</sup>. No CO<sub>2</sub> flux estimates were made for the tributary sampling sites, since both approaches would be hampered by a lack of adequate ancillary information - data on river depth and flow velocity are lacking, and the varying degree of canopy closure would compromise the use of modeled wind speed data.

For the analysis of δ<sup>13</sup>C<sub>DIC</sub>, a 2 mL helium (He) headspace was created, and H<sub>3</sub>PO<sub>4</sub> was added to convert all DIC species to CO<sub>2</sub>. After overnight equilibration, part of the headspace was injected into the He stream of an elemental analyser - isotope ratio mass spectrometer (EA-IRMS, ThermoFinnigan Flash HT and ThermoFinnigan DeltaV Advantage) for δ<sup>13</sup>C measurements. The obtained δ<sup>13</sup>C data were corrected for the isotopic equilibration between gaseous and dissolved CO<sub>2</sub> as described in Gillikin and Bouillon<sup>56</sup> and measurements were calibrated with certified reference materials LSVEC and either NBS-19 or IAEA-CO-1. Reproducibility of δ<sup>13</sup>C measurements was 0.2‰ or better. Concentrations of CH<sub>4</sub> and N<sub>2</sub>O were determined via the headspace equilibration technique (20 mL N<sub>2</sub> headspace in 50 mL serum bottles) and measured by gas chromatography (GC, 63) with flame ionization detection (GC-FID) and electron capture detection (GC-ECD) with a SRI 8610C GC-FID-ECD calibrated with CH<sub>4</sub>:CO<sub>2</sub>:N<sub>2</sub>O:N<sub>2</sub> mixtures (Air Liquide Belgium) of 1, 10 and 30 ppm CH<sub>4</sub> and of 0.2, 2.0 and 6.0 ppm N<sub>2</sub>O, and using the solubility coefficients of Yamamoto et al.<sup>57</sup> for CH<sub>4</sub> and Weiss and Price<sup>58</sup> for N<sub>2</sub>O.

25 mL filters for POC, PN and δ<sup>13</sup>C<sub>POC</sub> were decarbonated with HCl fumes for 4 h, re-dried and packed in Ag cups. POC, PN, and δ<sup>13</sup>C<sub>POC</sub> were determined on the





abovementioned EA-IRMS using the thermal conductivity detector (TCD) signal of the EA to quantify POC and PN, and by monitoring  $m/z$  44, 45, and 46 on the IRMS. An internally calibrated acetanilide and sucrose (IAEA-C6) were used to calibrate the  $\delta^{13}\text{C}_{\text{POC}}$  data and quantify POC and PN, after taking filter blanks into account. Reproducibility of  $\delta^{13}\text{C}_{\text{POC}}$  measurements was better than  $\pm 0.2\%$ . Samples for DOC and  $\delta^{13}\text{C}_{\text{DOC}}$  were analysed either on a Thermo HyperTOC-IRMS, or with an Aurora1030 TOC analyser (OI Analytical) coupled to a Delta V Advantage IRMS. Typical reproducibility observed in duplicate samples was in most cases  $< \pm 5\%$  for DOC, and  $\pm 0.2\%$  for  $\delta^{13}\text{C}_{\text{DOC}}$ . For a subset of samples from the Ngotto Forest, we compared DOC concentrations and  $\delta^{13}\text{C}$  data for samples filtered on  $0.2\ \mu\text{m}$  (as described above) and only on  $0.7\ \mu\text{m}$  GF/F filters; for both variables no significant differences were found ( $n=15$ , two-tailed paired t-test, in both cases  $p < 0.0001$  at 95% confidence interval, data in Supplementary Table 1).

Samples for major element concentrations and Si were filtered through a  $0.45\ \mu\text{m}$  polyethersulfone (PES) or polycarbonate (PC) filter, and measured by ICP-AES (Iris Advantage, Thermo) or ICP-MS (Perkin Elmer Elan 6100).

Samples for the analyses of cDOM spectral characteristics were prepared similarly as for DOC analyses, but without  $\text{H}_3\text{PO}_4$  addition. cDOM samples were stored in amber glass vials with PTFE-coated septa. Absorbance measurements were recorded on a Perkin-Elmer UV/Vis 650S using a  $1\ \text{cm}$  quartz cuvette. Absorbance spectra were measured from  $190$  to  $900\ \text{nm}$  at  $1\ \text{nm}$  increments and noise instrument was assessed measuring Milli-Q water as blank. The correction for scattering, index of refraction and blank was performed by fitting the absorption spectra to the data over the range  $200\text{--}700\ \text{nm}$  according to the following equation:

$$A_\lambda = A_0 e^{-S(\lambda - \lambda_0)} + K, \quad (1)$$

where  $A_\lambda$  and  $A_0$  are the absorbance measured at defined wavelength  $\lambda$  (nm) and at reference wavelength  $\lambda_0 = 375\ \text{nm}$ , respectively,  $S$  is the spectral slope ( $\text{nm}^{-1}$ ) that describes the approximate exponential decline in absorption with increasing wavelength, and  $K$  is a background offset. According to Johannessen and Miller<sup>59</sup>, the offset value was then subtracted from the whole spectrum. The fit was not used for any purpose other than to provide an offset value. After correction, absorption coefficients were calculated according to the relation:

$$a_\lambda = 2.303 \times A_\lambda / L, \quad (2)$$

where  $a_\lambda$  is the absorption coefficient ( $\text{m}^{-1}$ ) at wavelength  $\lambda$ ,  $A$  is the absorbance corrected at wavelength  $\lambda$ , and  $L$  the path length of the optical cell in meters ( $0.01\ \text{m}$ ).

Several optical indices were calculated to investigate CDOM properties, including spectral slopes over the ranges  $275\text{--}295\ \text{nm}$  ( $S_{275-295}$ ) and  $350\text{--}400\ \text{nm}$  ( $S_{350-400}$ ), the slope ratio (SR) and the  $a_{250}:a_{365}$  ratio. Spectral slopes were determined using linear regression for the log-transformed spectra for the intervals  $275\text{--}295\ \text{nm}$  and  $350\text{--}400\ \text{nm}$  and the slope ratio SR was calculated as the ratio of  $S_{275-295}$  to  $S_{350-400}$ <sup>22</sup>. The  $a_{250}:a_{365}$  ratio (also called E2:E3 ratio) was calculating using absorption coefficients at the appropriate wavelengths.

Literature data on specific parameters were obtained either from tabulated values in the relevant papers, data supplied by authors, or digitized from figures using PlotDigitizer v2.6.1 (<http://plotdigitizer.sourceforge.net/>).

- Cole, J. J. *et al.* Plumbing the global carbon cycle: Integrating inland waters into the terrestrial carbon budget. *Ecosystems* **10**, 171–184 (2007).
- Bastviken, D. *et al.* Freshwater methane emissions offset the continental carbon sink. *Science* **33**, 50 (2011).
- Raymond, P. A. *et al.* Global carbon dioxide emissions from inland waters. *Nature* **503**, 355–359 (2013).
- Ludwig, W., Probst, J. L. & Kempe, S. Predicting the oceanic input of organic carbon by continental erosion. *Global Biogeochem. Cycles* **10**, 23–41 (1996).
- Schlünz, B. & Schneider, R. R. Transport of terrestrial organic carbon to the oceans by rivers: re-estimating flux and burial rates. *Int. J. Earth Sci.* **88**, 599–606 (2000).
- Aufdenkampe, A. K. *et al.* Riverine coupling of biogeochemical cycles between land, oceans, and atmosphere. *Front. Ecol. Environ.* **9**, 53–60 (2011).
- Probst, J. L., Mortatti, J. & Tardy, Y. Carbon river fluxes and weathering  $\text{CO}_2$  consumption in the Congo and Amazon river basins. *Appl. Geochem.* **9**, 1–13 (1994).
- Négre, P. *et al.* Erosion sources determined by inversion of major and trace element ratios and strontium isotopic ratios in river water: the Congo Basin case. *Earth Planet. Sci. Lett.* **120**, 59–79 (1993).
- Seyler, P. & Elbaz-Poulichet, F. Biogeochemical control on the temporal variability of trace element concentrations in the Oubangui river (Central African Republic). *J. Hydrol.* **180**, 319–332 (1996).
- Coyne, A. *et al.* Spatial and seasonal dynamics of total suspended sediment and organic carbon species in the Congo River. *Glob. Biogeochem. Cycles* **19**, GB4019 (2005).
- Laraque, A. *et al.* A review of material transport by the Congo River and its tributaries. *Hydrol. Process.* **23**, 3216–3224 (2009).
- Seyler, P. *et al.* Concentrations, fluctuations saisonnières et flux de carbone dans le bassin du Congo. *Grands Bassins Fluviaux* (ORSTOM, Paris, 1995).
- Mariotti, A. *et al.* Carbon isotope composition and geochemistry of particulate organic matter in the Congo River (Central Africa): application to the study of Quaternary sediments off the mouth of the river. *Chem. Geol.* **86**, 345–357 (1991).

- Spencer, R. G. M. *et al.* Temporal controls on dissolved organic matter and lignin biogeochemistry in a pristine tropical river, Democratic Republic of Congo. *J. Geophys. Res.* **115**, G03013, doi:10.1029/2009JG001180 (2010).
- Spencer, R. G. M. *et al.* An initial investigation into the organic matter biogeochemistry of the Congo River. *Geochim. Cosmochim. Acta* **84**, 614–627 (2012).
- Wang, Z. A. *et al.* Inorganic carbon speciation and fluxes in the Congo River. *Geophys Res Lett* **40**, doi:10.1002/grl.50160 (2013).
- Bouillon, S. *et al.* Organic matter sources, fluxes and greenhouse gas exchange in the Oubangui River (Congo River basin). *Biogeosciences* **9**, 2045–2062; doi:10.5194/bg-9-2045-2012 (2012).
- Laraque, A. *et al.* Impact of lithological and vegetal covers on flow discharge and water quality of Congolese tributaries of the Congo River. *Rev. Sci. Eau* **11**, 209–224 (1998).
- Mann, P. J. *et al.* The biogeochemistry of carbon across a gradient of streams and rivers within the Congo Basin. *J. Geophys. Res.* doi:10.1002/2013JG002442 (in press).
- Richey, J. E. *et al.* Outgassing from Amazonian rivers and wetlands as a large tropical source of atmospheric  $\text{CO}_2$ . *Nature* **416**, 617–620 (2002).
- Mayorga, E. & Aufdenkampe, A. [Processing of bioactive elements in the Amazon River system]. *The Ecohydrology of South American Rivers and Wetlands* [McClain, M.E. (ed)] [1–24] (IAHS Press, Wallingford, UK, 2002).
- Helms, J. R. *et al.* Absorption spectral slopes and slope ratios as indicators of molecular weight, source, and photobleaching of chromophoric dissolved organic matter. *Limnol. Oceanogr.* **53**, 955–969 (2008).
- Peuravuori, J. & Pihlaja, K. Molecular size distribution and spectroscopic properties of aquatic humic substances. *Anal. Chim. Acta* **337**, 133–149 (1997).
- Spencer, R. G. M., Butler, K. D. & Aiken, G. R. Dissolved organic carbon and chromophoric dissolved organic matter properties of rivers in the USA. *J. Geophys. Res.* **117**, G03001, doi:10.1029/2011JG001928 (2012).
- Aiken, G. R. *et al.* Isolation of hydrophobic organic-acids from water using nonionic macroporous resins. *Org. Geochem.* **18**, 567–573 (1992).
- McKnight, D. M. & Aiken, G. R. [Sources and age of aquatic humus]. *Aquatic Humic Substances* [Hessen, D. & TranvikL. (eds)] [9–39] (Springer, Berlin, 1998).
- Cory, R. M. *et al.* Chemical characteristics of fulvic acids from Arctic surface waters: Microbial contributions and photochemical transformations. *J. Geophys. Res.* **112**, G04S51, doi:10.1029/2006JG000343 (2007).
- Spencer, R. G. M. *et al.* Utilizing chromophoric dissolved organic matter measurements to derive export and reactivity of dissolved organic carbon exported to the Arctic Ocean: A case study of the Yukon River, Alaska. *Geophys. Res. Lett.* **36**, L06401, doi:10.1029/2008GL036831 (2009).
- Yamashita, Y. *et al.* Optical characterization of dissolved organic matter in tropical rivers of the Guayana Shield, Venezuela. *J. Geophys. Res.* **115**, G00F10, doi:10.1029/2009JG000987 (2010).
- Mann, P. J. *et al.* Controls on the composition and lability of dissolved organic matter in Siberia's Kolyma River basin. *J. Geophys. Res.* **117**, G01028, doi:10.1029/2011JG001798 (2012).
- Hernes, J. P. *et al.* The role of hydrologic regimes on dissolved organic carbon composition in an agricultural watershed. *Geochim. Cosmochim. Acta* **72**, 5266–5277 (2008).
- Kohn, M. J. Carbon isotope compositions of terrestrial C3 plants as indicators of (paleo)ecology and (paleo)climate. *PNAS* **107**, 19691–19695 (2010).
- Cerling, T. E., Hart, J. A. & Hart, T. B. Stable isotope ecology of the Ituri Forest. *Oecologia* **138**, 5–12 (2004).
- Milliman, D. J. & Farnsworth, L. K. *River discharge to the coastal ocean: a global synthesis* (Cambridge University Press, 2011).
- Tamooh, F. *et al.* Distribution and origin of suspended matter and organic carbon pools in the Tana River Basin, Kenya. *Biogeosciences* **9**, 2905–2920; DOI:10.5194/bg-9-2905-2012 (2012).
- Meybeck, M. Carbon, nitrogen, and phosphorus transport by world rivers. *Am. J. Sci.* **282**, 401–450 (1982).
- Garrels, R. M. & Mackenzie, F. T. *Evolution of Sedimentary Rocks* (W.W. Norton, New York, 1971).
- Meybeck, M. Global chemical weathering of surficial rocks estimated from river dissolved loads. *Am. J. Sci.* **287**, 401–428 (1987).
- Gaillardet, J., Dupré, B. & Allègre, C. J. A global mass budget applied to the Congo Basin rivers: erosion rates and continental crust composition. *Geochim. Cosmochim. Acta* **59**, 3469–3485 (1995).
- Tamooh, F. *et al.* Dynamics of dissolved inorganic carbon and aquatic metabolism in the Tana River Basin, Kenya. *Biogeosciences* **10**, 6911–6928; DOI:10.5194/bg-10-6911-2013 (2013).
- Mook, W. G. & Tan, F. C. [Stable carbon isotopes in rivers and estuaries]. *Biogeochemistry of Major World Rivers* [Degens, E.T., Kempe, S. & Richey, J.E. (eds)] [245–264] (John Wiley, Hoboken, N. J., 1991).
- Mayorga, E. *et al.* Young organic matter as a source of carbon dioxide outgassing from Amazonian rivers. *Nature* **436**, 538–541 (2005).
- Ellis, E. E. *et al.* Factors controlling water-column respiration in rivers of the central and southwestern Amazon Basin. *Limnol. Oceanogr.* **57**, 527–540 (2012).
- Lauerwald, R. *et al.* What controls the spatial patterns of the riverine carbonate system? A case study for North America. *Chem. Geol.* **337–338**, 114–127 (2013).



45. Marwick, T. R. *et al.* Dynamic seasonal nitrogen cycling in response to anthropogenic N-loading in a tropical catchment, the Athi-Galana-Sabaki River, Kenya. *Biogeosciences* **11**, 443–460; DOI:10.5194/bg-11-443-2014 (2014).
46. Koné, Y. J. M. *et al.* Seasonal variability of methane in the rivers and lagoons of Ivory Coast (West Africa). *Biogeochemistry* **100**, 21–37 (2010).
47. Bouillon, S. *et al.* Distribution, origin and cycling of carbon in the Tana River (Kenya): a dry season basin-scale survey from headwaters to the delta. *Biogeosciences* **6**, 2475–2493; DOI:10.5194/bg-6-2475-2009 (2009).
48. Baulch, H. M. *et al.* Nitrogen enrichment and the emissions of nitrous oxide from streams. *Glob. Biogeochem. Cycles* **25**, GB4013 (2011).
49. Regnier, P. *et al.* Anthropogenic perturbation of the carbon fluxes from land to ocean. *Nature Geosc* **6**, 597–607 (2013).
50. Duveiller, G. *et al.* Deforestation in Central Africa: estimates at regional, national and landscape levels by advanced processing of systematically-distributed Landsat extracts. *Remote Sens. Environm.* **112**, 1969–1981 (2008).
51. Brugière, D., Sakom, D. & Gautier-Hion, A. The conservation significance of the proposed Mbaéré-Bodingué national park, Central African Republic, with special emphasis on its primate community. *Biodiversity and Conservation* **14**, 505–522 (2005).
52. Milesi, J. P. *et al.* An overview of the geology and major ore deposits of Central Africa: Explanatory note for the 1:4,000,000 map “Geology and major ore deposits of Central Africa”. *J. Afr. Earth Sci.* **44**, 571–595 (2006).
53. Abril, G., Commarieu, M. V. & Guérin, F. Enhanced methane oxidation in an estuarine turbidity maximum. *Limnol. Oceanogr.* **52**, 470–475 (2007).
54. Millero, F. J. The thermodynamics of the carbonic acid system in seawater. *Geochim. Cosmochim. Acta* **43**, 1651–1661 (1979).
55. Lewis, E. & Wallace, D. W. R. *Program developed for CO<sub>2</sub> system calculations* (Carbon Dioxide Information Analysis Center, Oak Ridge National Laboratory, U.S. Department of Energy, Oak Ridge, Tennessee, 1998). Available online at <http://cdiac.ornl.gov/oceans/co2rprt.html>, accessed February 2014.
56. Gillikin, D. P. & Bouillon, S. Determination of  $\delta^{18}\text{O}$  of water and  $\delta^{13}\text{C}$  of dissolved inorganic carbon using a simple modification of an elemental analyzer – isotope ratio mass spectrometer (EA-IRMS): an evaluation. *Rapid Comm. Mass Spectrom.* **21**, 1475–1478 (2007).
57. Weiss, F. R. & Price, B. A. Nitrous oxide solubility in water and seawater. *Mar. Chem.* **8**, 347–359 (1980).
58. Yamamoto, S., Alcauskas, J. B. & Crozier, T. E. Solubility of methane in distilled water and seawater. *J. Chem. Eng. Data* **21**, 78–80 (1976).
59. Johannessen, S. C. & Miller, W. L. Quantum yield for the photochemical production of dissolved inorganic carbon in seawater. *Mar. Chem.* **76**, 271–283 (2001).

## Acknowledgments

This work was financially supported by the European Research Council (StG 240002: AFRIVAL: “African river basins: catchment-scale carbon fluxes and transformations”), two travel grants to S.B. from the Research Foundation Flanders (FWO-Vlaanderen), and a National Geographic Society Research and Exploration Grant (#8885-11) to D.P.G. and S.B. We thank Marc-Vincent Commarieu for analyses of TA, Zita Kelemen for IRMS support, Harold Hughes (Museum for Central Africa, Tervuren, Belgium) and Kristin Coorevits (KU Leuven) for ICP-MS analyses, and Christiane Lancelot for access to the Perkin-Elmer UV/Vis 650S. A.V.B. and T.L. are a senior research associate and postdoctoral researcher, respectively, with the Fonds National de la Recherche Scientifique (FNRS, Belgium). We thank all staff members of the ECOFAC (Ecosystemes Forestiers d’Afrique Centrale) centre in Ngotto for their hospitality and assistance in the field, in particular Denis Passy. A. Coynel and A. Wang kindly provided the raw data of their published work. J. Hartmann and Nils Moosdorf kindly shared their knowledge concerning the lithology of the study catchments.

## Author contributions

S.B. and A.V.B. designed the research; S.B., A.Y. and D.P.G. conducted the field sampling, S.B., A.V.B., T.L., C.T. and F.D. analysed samples, S.B. drafted the manuscript with input from A.V.B., A.Y., D.P.G., T.L., C.T. and F.D.

## Additional information

**Supplementary information** accompanies this paper at <http://www.nature.com/scientificreports>

**Competing financial interests:** The authors declare no competing financial interests.

**How to cite this article:** Bouillon, S. *et al.* Contrasting biogeochemical characteristics of the Oubangui River and tributaries (Congo River basin). *Sci. Rep.* **4**, 5402; DOI:10.1038/srep05402 (2014).



This work is licensed under a Creative Commons Attribution-NonCommercial-NoDerivs 4.0 International License. The images or other third party material in this article are included in the article’s Creative Commons license, unless indicated otherwise in the credit line; if the material is not included under the Creative Commons license, users will need to obtain permission from the license holder in order to reproduce the material. To view a copy of this license, visit <http://creativecommons.org/licenses/by-nc-nd/4.0/>